

Reset Controller Synthesis by Reach-avoid Analysis for Delay Hybrid Systems

Han Su ^a, Jiyu Zhu ^a, Shenghua Feng ^a, Yunjun Bai ^b, Bin Gu ^b, Jiang Liu ^c,
Mengfei Yang ^d, Naijun Zhan ^a

^a*Institute of Software, University of Chinese Academy of Sciences, Beijing, China*

^b*Beijing Institute of Control Engineering, Beijing, China*

^c*Chongqing Institute of Green and Intelligent Technology, Chinese Academy of Sciences, Chongqing, China*

^d*China Academy of Space Technology, Beijing, China*

Abstract

A reset controller plays a crucial role in designing hybrid systems. It restricts the initial set and redefines the reset map associated with discrete transitions, in order to guarantee the system to achieve its objective. Reset controller synthesis, together with feedback controller synthesis and switching logic controller synthesis, provides a correct-by-construction approach to designing hybrid systems. However, time-delay is an inevitable factor in hybrid systems, which can degrade control performance and render verification certificates obtained by abstracting away time-delay invalid in practice. In this paper, we investigate this issue in a practical manner by taking time-delay into account. We propose an approach that reduces the synthesis of reset controllers to the generation of reach-avoid sets for the hybrid system under consideration, which can be efficiently solved using off-the-shell convex optimization solvers.

Key words: Delay Hybrid systems, reset controllers, delay differential equations, reach-avoid sets

1 Introduction

In the past two decades, embedded systems have experienced significant advancements and have become increasingly interconnected. This integration has fostered deep interaction between computation, communication, and control, giving rise to the emergence of hybrid systems (HS). HS are characterized by the interaction between continuous-time and discrete-event dynamics. The correct design of reliable HS is a crucial research issue, especially in safety-critical domains such as health care and medicine [12], autonomous vehicles [10], and automated factories [40]. Controller synthesis plays a vital role in ensuring that HS meet specified safety and/or liveness requirements. However, due to the inherent complexity of HS, controller synthesis is a notoriously challenging field that has attracted increasing

attention in recent years.

Controller synthesis offers a correct-by-construction manner that can algorithmically construct an operational behavior model to ensure the execution of a considered HS satisfying its specification, such as safety and reach-avoid properties. Three commonly employed control mechanisms for HS are *feedback controller* [9], *switching logic controller* [5] and *reset controller* [11]. Feedback controllers are typically used to ensure the stability of HS by updating inputs impeded on its dynamics [9]. Switching logic controllers allow achieving various control specifications by redesigning the guard condition associated with each jump and the domain constraint in each mode of the considered HS. However, in some scenarios, such as when part of the initial condition and/or the range of the reset map of the considered HS are unsafe, feedback and switching logic controller may not work any more. In such cases, a reset controller, by redesigning the reset map and initial condition, provides an effective solution.

Reset controller synthesis is surprisingly overlooked in the literature, and even worse, most of existing work

Email addresses: suhan@ios.ac.cn (Han Su), zhuji@ios.ac.cn (Jiyu Zhu), fengsh@ios.ac.cn (Shenghua Feng), baiyj@ios.ac.cn (Yunjun Bai), gubinbj@sina.com (Bin Gu), liujiang@cigit.ac.cn (Jiang Liu), yangmf@bice.org.cn (Mengfei Yang), znj@ios.ac.cn (Naijun Zhan).

assume delay-free. However, in modern control, delays are inevitable due to various factors, for example, conversions between analog and digital signal domains, the presence of complex digital signal-processing chains for enhancing, filtering and fusing sensory signals before they enter control, sensor networks harvesting multiple sensor sources before feeding them to control, and network delays in networked control applications physically removing the controllers from the control path, and just name a few. The assumption of delay-free simplifies the problem mathematically, but is physically impossible and impractical. In reality, the presence of delays can lead to deteriorated control performance and render verification certificates obtained by abstracting away time-delay invalid in practice. This issue has been extensively discussed [6, 14, 42].

For example, consider a vehicle equipped with Mecanum wheels [13] that is moving horizontally, as indicated by the black arrow in the left part of Fig. 1. The vehicle has the capability to switch to vertical motion without relying on traditional steering mechanisms. So, its behaviour can be represented as a hybrid automaton shown in the right part of 1. In practice, obviously the vehicle samples data periodically by its sensors and takes time to switch between the two modes. Suppose the vehicle switches to vertical motion at a specific time t . Thus, if we abstract away the two types delays, then the position received by the controller before this discrete transition is at the position of the blue vehicle. While the actual position at time t is at the position of the orange one. So, if we apply a reset map without considering the delay, it may steer the vehicle to move upward, resulting in a collision with the black box (unsafe area). In fact, only a reset map guides the vehicle downward that can ensure the safety, see the green vehicle in Fig. 1.

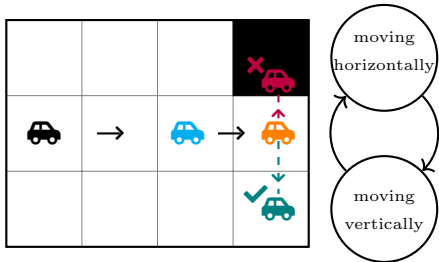


Fig. 1. A motivating example

A practical approach to designing reset controllers is to consider HS with delays. Generally, two types of delays can arise: one lies in continuous evolution and the other in discrete transitions between modes. The time-delay in continuous evolution is typically represented by delay differential equations (DDE), while the delay caused by a discrete transition can be viewed as the time taken by the jump. Delay hybrid automata, introduced in [6], is an appropriate model for capturing HS with both types of delays.

In this paper, we present our investigation into the synthesis of reset controllers for delay hybrid systems (dHS)

that exhibit delays in both continuous evolution and discrete transitions. The reset map associated with a discrete transition is typically a set-valued function that defines the relationship between continuous evolution in the post-mode and the previous mode. Our objective is to synthesize a reset map that guarantees the satisfaction of both safety and liveness conditions for dHS. Specially, we aim to find a reset map that ensures all executions of dHS can eventually reach a target set T while remaining within a safe set S before reaching T . We tackle this problem in three steps. Firstly, we propose a novel reach-avoid analysis method for DDEs by introducing a reach-avoid barrier functional (RABFal). We demonstrate that RABFal can be synthesized by solving a reduced *semidefinite programming* (SDP) problem [36]. The 0-sublevel set of RABFal provides an inner-approximation of the reach-avoid set. Secondly, using the reach-avoid analysis method in the first step, we propose a mode partition algorithm to partition each mode of dHS into several sub-modes, each with a unique type of execution. Then we abstract the resulted dHS into a discrete directed graph (DDG) by discarding the continuous dynamics. Finally, we identify and block edges that may lead to “non-target sink” or “infinite loop” based on the obtained DDG in the second step, where the dHS fails to reach the target set. Finally, based on the results obtained after edge blocking, we synthesize a reset controller to guarantee safety and liveness for dHS. Experimental results on examples from the literature demonstrate the effectiveness of our approach.

In summary, our main contribution are as follows.

- We propose a novel method for reach-avoid analysis of DDE, achieving a better performance than existing methods.
- We introduce an efficient algorithm to synthesize reset controller for dHS by reduction to the problem of reach-avoid analysis for continuous dynamics and depth-first-search with block for discrete-event dynamics.
- We provide a prototypical implementation of our approach and apply it to several case studies to illustrate the effectiveness and efficiency of our approach.

Related work A wide range of mathematical models, including finite state automaton and various types of differential equations, are employed to reason about the rich behavior of HS [30]. In the realm of formal verification for HS, controller synthesis is a correct-by-construct manner providing mathematical guarantees for the correctness and reliability of HS. Extensive research has been conducted on this problem, leading to the development of various approaches to feedback controllers, switching logic controllers, and reset controllers.

Feedback controllers play a crucial role in guiding the continuous behaviors of HS towards equilibrium points or away from unsafe regions. A feedback controller computes inputs based on the system state to modulate the physical disciplines of the continuous evolution. A de-

tailed introduction to this issue can be found in [32]. Various methods have been proposed for feedback controller synthesis. These include multiple Lyapunov function based methods [9], moment based methods [41], Hamilton-Jacobi based methods [35], Barrier certificates based methods [3], abstraction-based methods [18, 33], and counter-examples guided inductive synthesis methods [1], and so on.

Switching logic controllers refine the domain constrain for each mode and guard condition for each discrete transition to modify the behavior of HS in order to satisfy given specifications. In the literature, switching logic synthesis has been extensively studied, and various approaches have been proposed. These approach can be categorized into abstraction-based methods [8, 18, 22, 26, 31, 33] and constraint solving based methods [34, 39].

Reset controllers refine the set of initial states associated with each mode and modify the reset map associated with each discrete transition to ensure that any execution of the considered HS satisfies the given specification. The investigation of reset controllers was initially introduced by Clegg in 1958 [11] as a means to overcome the limitations of linear control. A comprehensive introduction to reset controllers can be found in [29]. Although there has been some work on reset controller synthesis, most of it primarily focus on stability analysis for systems without delays [7, 20]. To the best of our knowledge, our paper is the first work on reset controller synthesis for dHS.

Reach-avoid analysis serves as a vital tool for the reset controller synthesis algorithm presented in this paper. Existing works in the literature, as surveyed by [15], have primarily focused on reach-avoid analysis for ordinary differential equations (ODEs). However, for systems that incorporate delays, alternative approaches have been proposed. For instance, [23] proposed a time-bounded invariant verification method that analyzes the sensitivity of trajectories with respect to the initial states and inputs of the system. [38] introduced a reachable set approximation method for DDE that features a local homeomorphism property. In recent years, there has been a growing interest in methods based on computing barrier certificates. [27] introduced the concept of barrier functional for DDE, [24] proposed a barrier functional for safety critical control of DDE, [37] proposed a barrier function based method for reach-avoid analysis. Despite numerous methods proposed for reach-avoid analysis, previous works have not explored the use of *barrier functionals* extensively. This may be due to the challenge of finding a balance between solvability and expressiveness of the associated constraints. In this paper, we address this challenge specifically for polynomial delay differential equations.

Organization. In the following, Sect. 2 provides a recap of important preliminary definitions and formally defines the problem of interest. Sect. 3 presents our reach-avoid analysis method by introducing reach-avoid

barrier functional, Sect. 4 proposes a mode partition algorithm based on the novel reach-avoid analysis method. Additionally, we describe a method to abstract the dHA after partitioning it into a DDG. Sect. 5 introduces a depth-first-search algorithm for modifying the DDG after the abstraction process. In Sect. 6, we demonstrate the effectiveness of our method through several examples. Finally, we conclude the paper in Sect. 7.

2 Preliminaries and Problem Formulation

Notations \mathbb{R} denotes the set of real numbers, while $\mathbb{R}_{\geq 0}$ denotes the set of non-negative real numbers. \mathbb{R}^n denotes the n -dimensional real Euclidean space. $\mathcal{C}([-\tau, 0], \mathbb{R}^n)$ denotes the Banach space of continuous functions that map the interval $[-\tau, 0]$ to \mathbb{R}^n , equipped with the norm $\|\mathbf{x}_t\|_{\mathcal{C}} = \max_{\theta \in [-\tau, 0]} \|\mathbf{x}_t(\theta)\|$, where $\|\cdot\|$ represents the Euclidean norm. For a set A , ∂A represents its boundary, and $\mathcal{P}(A)$ represents its power set. $\mathbb{R}[\mathbf{x}]$ denotes the polynomial ring in \mathbf{x} over the field \mathbb{R} . A polynomial $h \in \mathbb{R}[\mathbf{x}]$ is said to be *sum-of-squares* (SOS) if there exist polynomials $g_0, \dots, g_k \in \mathbb{R}[\mathbf{x}]$ such that $h = \sum_{i=0}^k g_i^2$. We denote by $\Sigma[\mathbf{x}] \subset \mathbb{R}[\mathbf{x}]$ the set of SOS polynomials over \mathbf{x} . $\mathbb{R}[\mathbf{x}]^n$ denotes the set of n -dimensional vectors, where each element is a polynomial in \mathbf{x} over the field \mathbb{R} . Similarly, $\Sigma[\mathbf{x}]^n$ represents the set of vectors of SOS polynomials. All vectors in this article are considered as column vectors by default, and A^T denotes the transpose of the matrix A . For a given vector \mathbf{u} , $|\mathbf{u}|$ denotes coordinate-wise absolute value of \mathbf{u} .

2.1 Delay Differential Equation

The system of interest in this paper is a time-delay hybrid system, where the dynamics in each mode is described by delay differential equations (DDEs) of the form:

$$\dot{\mathbf{x}}(t) = \mathbf{f}(\mathbf{x}(t), \mathbf{x}(t - \tau)), \quad \mathbf{f} \in \mathbb{R}[\mathbf{x}(t), \mathbf{x}(t - \tau)]^n \quad (1)$$

with domain $D \subseteq \mathbb{R}^n$, in which $\dot{\mathbf{x}}(t)$ denotes the derivative of $\mathbf{x}(t)$ with respect to t .

Unlike ODEs, the evolution of DDEs not only depends on the current state (cf. $\mathbf{x}(t)$), but also the previous state (cf. $\mathbf{x}(t - \tau)$). Thus, we interpret the state of DDEs as a function, not a point in \mathbb{R}^n .

A function $\mathbf{x}^\phi(\cdot) : \mathbb{R} \rightarrow \mathbb{R}^n$ is considered a solution of Eq. (1) with the initial function $\phi \in \mathcal{C}([-\tau, 0], D)$ if there exists a scalar $a > 0$ such that $\mathbf{x}^\phi(t)$ satisfying Eq. (1) for $t \in [-\tau, a)$. To ensure the existence and uniqueness of the solution, we assume \mathbf{f} is *locally Lipschitz*.

Thus, the state of Eq. (1) at time t is represented by the continuous function $\mathbf{x}_t^\phi(\cdot)$ defined over the interval $[-\tau, 0]$ as follow:

$$\mathbf{x}_t^\phi(\theta) = \mathbf{x}^\phi(t + \theta), \quad \theta \in [-\tau, 0], \mathbf{x}(\cdot) \in D \subseteq \mathbb{R}^n$$

Intuitively, the state of DDEs at time t encodes the trajectory over the interval $[t - \tau, t]$ and allows for further evolution of the solution. In the notation, we may omit

initial condition ϕ in the state $\mathbf{x}_i^\phi(\cdot)$ and solution $\mathbf{x}^\phi(t)$ when it is clear from the context.

2.2 Delay Hybrid Automata

Hybrid automata (HA) are widely used mathematical models for describing the behavior of HS. To capture delays in HS, a variant called *delay hybrid automata* (dHA) was introduced in [6]. dHA extends the concept of HA by incorporating both discrete and continuous delays. We will employ dHA as the underlying model of dHA in this paper. Formally,

Definition 1 (Delay Hybrid Automata [6]) A *delay hybrid automaton*, denoted as $\mathcal{H} = (Q, X, Dom, F, Init, E, G, ST, R)$, is defined as a tuple consisting of the following components:

- $Q = \{q_1, q_2, \dots, q_m\}$ is a finite set of modes;
- $X \subseteq \mathbb{R}^n$ is the set of instant continuous state;
- $Dom(\cdot) : Q \rightarrow \mathcal{P}(X)$ assigns each mode a domain that system evolves within.
- $F = \{\mathbf{f}_1, \mathbf{f}_2, \dots, \mathbf{f}_m\}$ is the set of vector fields corresponding to modes q_1, q_2, \dots, q_m . For each mode q_i , the continuous evolution is described by a DDE of the form:

$$\dot{\mathbf{x}}(t) = \mathbf{f}_i(\mathbf{x}(t), \mathbf{x}(t - \tau));$$

- $Init(\cdot) : Q \rightarrow \mathcal{C}([t_1, t_2], X)$, where $t_1 \leq t_2$, associates each mode with a set of initial functions representing the possible initial states;
- $E \subseteq Q \times Q$ defines a set of discrete transitions, also called edges, between modes¹;
- $G(\cdot) : E \rightarrow \mathcal{P}(X)$ specifies the guard condition for each discrete transition;
- $ST(\cdot) : E \rightarrow \mathbb{R}_{\geq 0}$ indicates the time consumed by each discrete transition.
- $R(\cdot, \cdot) : E \times X \rightarrow \mathcal{P}(\mathcal{C}([t_1, t_2], X))$ defines the reset map for each edge $e = (q_1, q_2)$ from an instant continuous state $x \in \mathbb{R}^n$ in its pre-mode q_1 into the set of initial functions in its post-mode q_2 .

For a given dHA \mathcal{H} , we refer to tuple $(q(t), \mathbf{x}(t)) \in Q \times X$ as the *instant state* of \mathcal{H} at time t . Here, $q(t)$ represents the mode, and $\mathbf{x}(t)$ for the instant continuous state of \mathcal{H} at time t .

Remark 1 Note that an instant continuous state of \mathcal{H} is an element of \mathbb{R}^n , whereas a state of DDE is a function in $\mathcal{C}([-\tau, 0], \mathbb{R}^n)$. Actually, an instant continuous state $\mathbf{x}(t)$ of \mathcal{H} in a mode q_i can be interpreted as the value of the state $\mathbf{x}_t(\cdot)$ of the corresponding DDE with the vector field f_i at the endpoint, i.e., $\mathbf{x}(t) = \mathbf{x}_t(0)$.

Different from the definition of HA, there are several notable changes in Def. 1:

1. As discussed in Sect. 2.1, the initial set $Init(q) \subseteq \mathcal{C}([t_1, t_2], Dom(q))$ for each mode q consists of functions;
2. A discrete transition e may have a time duration, denoted by $ST(e)$;
3. The reset map $R(e, \mathbf{x})$ in dHA maps an instant continuous state $\mathbf{x} \in \mathbb{R}^n$ in the pre-mode of edge $e = (p, q)$,

¹ For an edge $e = (q, p)$ in dHA, we call q the pre-mode of e while p the post-mode of e .

satisfying $G(e)$, to a set of states in the post-mode. These states are represented as continuous functions $R(e, \mathbf{x}) \subseteq \mathcal{C}([t_1, t_2], Dom(q))$.

Example 2 Consider a hybrid linear damped oscillator that exhibits the ability to switch between different damping ratios. We model it as a dHA given in Fig. 2, and will use it as a running example throughout the paper.

- $Q = \{q_1, q_2, q_3\}$;
- $X = \{(x_1, x_2) \mid x_1^2 + x_2^2 - 1 \leq 0\}$;
-

$$Dom(q_1) = \left\{ (x_1, x_2) \mid \begin{array}{l} x_1^2 + x_2^2 \leq 1 \wedge x_1^2 + x_2^2 \geq 0.1 \wedge \\ (x_1 + 0.3)^2 + (x_2 + 0.3)^2 \geq 0.1 \end{array} \right\}$$

$$Dom(q_2) = \{(x_1, x_2) \mid x_1^2 + x_2^2 \leq 1\}$$

$$Dom(q_3) = \left\{ (x_1, x_2) \mid \begin{array}{l} (x_1 - 0.5)^2 + (x_2 - 0.5)^2 \geq 0.1 \\ \wedge x_1^2 + x_2^2 \leq 1 \end{array} \right\}$$

- $F = \{\mathbf{f}_1, \mathbf{f}_2, \mathbf{f}_3\}$, where

$$\mathbf{f}_1 = \begin{cases} 0.5x_2(t) + 0.5x_2(t - 0.1), \\ -0.5x_1(t) - 0.5x_1(t - 0.1) - 1.5x_2(t), \end{cases}$$

$$\mathbf{f}_2 = \begin{cases} 0.88x_2(t) + 0.12x_2(t - 1), \\ -0.88x_1(t) - 0.12x_1(t - 1) - 1.5x_2(t), \end{cases}$$

$$\mathbf{f}_3 = \begin{cases} 0.6x_2(t) + 0.4x_2(t - 0.2), \\ -0.6x_1(t) - 0.4x_1(t - 0.2) - 1.5x_2(t); \end{cases}$$

- $Init(q_1) = \mathcal{C}([-0.1, 0], Dom(q_1))$, $Init(q_2) = Init(q_3) = \emptyset$
- $E = \{e_1 = (q_1, q_2), e_2 = (q_1, q_3), e_3 = (q_3, q_1)\}$;
- $G(e_1) = \{(x_1, x_2) \mid x_1^2 + x_2^2 - 0.1 \leq 0\}$,
- $G(e_2) = \{(x_1, x_2) \mid (x_1 + 0.3)^2 + (x_2 + 0.3)^2 - 0.1 \leq 0\}$,
- $G(e_3) = \{(x_1, x_2) \mid (x_1 - 0.5)^2 + (x_2 - 0.5)^2 - 0.1 \leq 0\}$;
- $ST(e_i) = 1, i = 1, 2, 3$;
- $R(e_1, (x_1, x_2)) = \mathcal{C}([-1, 0], Dom(q_2))$,
- $R(e_2, (x_1, x_2)) = \mathcal{C}([-0.2, 0], Dom(q_3))$,
- $R(e_3, (x_1, x_2)) = \mathcal{C}([-0.1, 0], Dom(q_1))$.

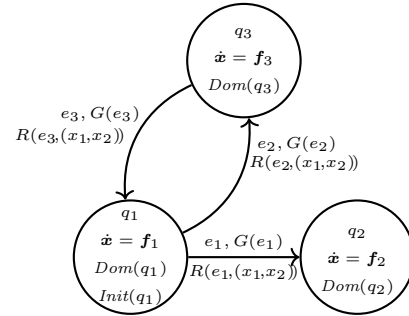


Fig. 2. The dHA for hybrid linear damped oscillator

◁

Definition 3 (Hybrid Execution) A *hybrid execution* π of dHA \mathcal{H} is a sequence of triple $\langle (I_i, q_i, \mathbf{x}^{\phi_i}(t)) \rangle$ for $i \in \mathbb{N}$ and $I_i = [t_i, t'_i]$ such that $t'_i \geq t_i$. This sequence satisfies the following conditions:

- *initial condition:* $\phi_0 \in Init(q_0)$;

- *discrete transition*: $e = (q_i, q_{i+1}) \in E$, $t_{i+1} = t'_i + ST(e)$, $\mathbf{x}^{\phi_i}(t'_i) \in G(e)$, $\phi_{i+1} \in R(e, \mathbf{x}^{\phi_i}(t'_i))$, $q(t) = q_i$ and $\mathbf{x}(t) = \mathbf{x}^{\phi_i}(t'_i)$ for $t \in [t'_i, t_{i+1})$.
- *continuous evolution*: (a) $q(t) \equiv q_i$ for all $t \in I_i$, (b) $\mathbf{x}^{\phi_i}(t)$ is the solution of $DDE \dot{\mathbf{x}}(t) = \mathbf{f}_i(\mathbf{x}(t), \mathbf{x}(t-\tau_i))$ with initial condition defined by ϕ_i , and (c) $\mathbf{x}^{\phi_i}(t) \in \text{Dom}(q_i)$.

Notice that an execution is required to remain in the domain throughout its continuous evolution, *except* at the time instants where a discrete transition happens. In addition, a discrete transition may take time, i.e., $ST(e) > 0$. In this case, the instant state remains unchanged during the time period except at the endpoint. An execution π is called *finite* if it is a finite sequence ending with a closed time interval. Otherwise, the execution π is called *infinite*. A dHA \mathcal{H} is called *non-blocking* if for any initial state $\phi \in \text{Init}(\cdot)$, there exists an infinite execution starting from ϕ . It is called *deterministic* if for any initial state ϕ there exists at most one execution starting from it.

Example 4 Let us continue Example 2.

$$\langle ([0, 3], q_1, \mathbf{x}^{\phi_1}(t)), ([4, 7], q_3, \mathbf{x}^{\phi_2}(t)), \dots \rangle,$$

is an execution of dHA in Fig 2, in which $\mathbf{x}^{\phi_1}(t)$ represents the solution of the DDE defined by \mathbf{f}_1 with an initial function $\phi_1 \in \text{Init}(q_1)$. Similarly, $\mathbf{x}^{\phi_2}(t)$ represents the solution of the DDE defined by \mathbf{f}_3 with an initial function ϕ_2 obtained from the reset map $R(e_1, (x_1, x_2))$.

The execution starts in mode q_1 and remains in this mode until $t = 3$ when the guard condition $G(e_1)$ is satisfied. However, there is a time delay $ST(e_1) = 1$ incurred by the edge e_1 . During the time interval $[3, 4)$, the instant state remains unchanged, i.e., $(q_1, \mathbf{x}^{\phi_0}(3))$. The discrete transition is completed at $t = 4$, and the execution continues in mode q_2 . The execution in q_2 continuous until $t = 7$, at which another discrete transition occurs. \triangleleft

Remark 2 In HA, there are two types of infinite executions: one type refers to executions with unbounded execution time, i.e., $\sum_{i=0}^N I_i = \infty$; the other involves bounded execution time but an infinite number of discrete transitions, known as Zeno. However, in dHA, the presence of switching time implies that infinite discrete transitions inevitably result in unbounded execution time, thereby preventing executions of type Zeno, except for the special case when all switching times are 0, i.e., dHA is degenerated to HA.

With the above definitions and notations, we define the reachable set of dHA in a standard way.

Definition 5 (Reachable Set) An instant state (q, \mathbf{x}) of dHA is called reachable if there exists a finite execution ending in (q, \mathbf{x}) . For a given dHA \mathcal{H} , the reachable set $\mathcal{R}_{\mathcal{H}}$ is defined as

$$\mathcal{R}_{\mathcal{H}} = \left\{ (q, \mathbf{x}) \left| \begin{array}{l} \exists \pi = \langle (I_0, q, \mathbf{x}^{\phi_0}(t)), \dots, (I_i, q_i, \mathbf{x}^{\phi_i}(t)) \rangle, \\ s.t. q = q_i, \exists t \in I_i, \mathbf{x} = \mathbf{x}^{\phi_i}(t) \end{array} \right. \right\}$$

2.3 Problem Formulation

Given a dHA \mathcal{H} as Def. 1 and a set of instant states S , and let $S_q = \{ \mathbf{x} \mid (q, \mathbf{x}) \in S \}$ for simplicity. We say \mathcal{H} is *safe* with respect to S , if for any reachable instant state (q, \mathbf{x}) , $(q, \mathbf{x}) \in S$ holds. We will try to solve the problem below:

Problem 1 Given a dHA \mathcal{H} as Def. 1, a compact safe set $S \subseteq Q \times X$ and target set $T \subseteq Q \times X$, whether can we find a new Init^r and R^r such that all executions of the modified dHA $\mathcal{H}^r = (Q, X, \text{Dom}, F, \text{Init}^r, E, G, ST, R^r)$ will reach the target set T while keeping safe before?

3 Reach-avoid Analysis in One Mode

Problem 1 essentially corresponds to the reach-avoid problem of \mathcal{H} . Therefore, we need to investigate the reach-avoid problem in each mode first, corresponding to the reach-avoid problem of DDE. This step serves as the first step of our approach.

In the context of DDEs, a reach-avoid set \mathcal{RA} is a set of initial functions, from which all trajectories must stay in the safe set S before eventually entering the target set T . In practice, the maximal reach-avoid set is more important, defined as follows

$$\mathcal{RA} := \left\{ \phi \in \mathcal{C}([- \tau, 0], S) \left| \begin{array}{l} \exists t' \in \mathbb{R}_{\geq 0}, \mathbf{x}^{\phi}(t') \in T \wedge \\ \forall t \in [- \tau, t'), \mathbf{x}^{\phi}(t) \in S \end{array} \right. \right\} \quad (2)$$

As a convention, in the rest of this paper, any reach-avoid set will refer to the corresponding maximal reach-avoid set if no otherwise stated.

Thus, the reach-avoid problem for DDE of the form Eq. (1) can be defined as below:

Problem 2 Given $S \subseteq D$ a compact set of safe instant states and $T \subseteq D$ a compact set of target instant states, we aim to inner-approximate the reach-avoid set \mathcal{RA} .

In what follows, we explain our reset controller synthesis algorithm to a fixed mode (say q_i) first, which can be essentially achieved through exploiting the solution to Problem 2.

3.1 Reach-Avoid Barrier Functional

In order to inner-approximate \mathcal{RA} more precisely, inspired by [24] and [37], we propose the notion of *reach-avoid barrier functional* (RABFal), whose 0-sublevel set provides an inner-approximation of \mathcal{RA} . Formally,

Definition 6 (Reach-Avoid Barrier Functional) Given DDE in the form of (1) with domain $D \subseteq \mathbb{R}^n$, safe set S and target set T defined by

$$S := \{ \mathbf{x} \in D \mid s(\mathbf{x}) \leq 0 \}, T := \{ \mathbf{x} \in D \mid g(\mathbf{x}) \leq 0 \},$$

we call $H : \mathcal{C}([- \tau, 0], D) \rightarrow \mathbb{R}$ a reach-avoid barrier functional if we can find a bounded function $w : D \rightarrow \mathbb{R}$ such that the following conditions are satisfied:

$$-\frac{dH(\mathbf{x}_t)}{dt} \geq 0, \forall \mathbf{x}_t \in \mathcal{C}([-\tau, 0], S), \quad (3)$$

$$H(\mathbf{x}_t) \geq 0, \forall \mathbf{x}_t \in \mathcal{C}([-\tau, 0], S), \text{ s.t. } \mathbf{x}_t(0) \in \partial S, \quad (4)$$

$$H(\mathbf{x}_t) - \frac{dw(\mathbf{x}_t(0))}{dt} \geq g(\mathbf{x}_t(0)), \forall \mathbf{x}_t \in \mathcal{C}([-\tau, 0], S). \quad (5)$$

Def. 6 generalizes the existing notion of reach-avoid barrier functions over instant states $\mathbf{x}_t(0) \in \mathbb{R}^n$ [37] to over function states \mathbf{x}_t . Intuitively, Cond. (3) together with Cond.(4) ensure that the trajectories starting from the 0-sublevel set of H will never leave the safe set. Additionally, Cond. (5), which involves the auxiliary function w , ensures that the trajectories starting from the 0-sublevel set of H will eventually enter the target set as the system evolves.

This generalization allows for an inner-approximation of the reach-avoid set using a Lyapunov-Krasovskii functional-like approach [16], which can provide a less conservative analysis of stability for DDEs. Previous methods, such as the one proposed in [37], consider the history term $\mathbf{x}(t - \tau)$ as a disturbance within an n -dimensional ball, where the ball's radius is determined by the delay τ and the Lipschitz constant of vector field \mathbf{f} . However, this approach is only applicable to DDEs with relatively small delays τ . In what following, we will provide examples (Example 9) to illustrate this limitation.

Theorem 7 *Given a DDE of the form (1) with domain $D \subseteq \mathbb{R}^n$, safe set S and target set T , if $H : \mathcal{C}([-\tau, 0], D) \rightarrow \mathbb{R}$ is a reach-avoid barrier functional, then the set \mathcal{RA}_{in} defined by the 0-sublevel set of H , i.e.,*

$$\mathcal{RA}_{in} := \{\phi \in \mathcal{C}([-\tau, 0], S) \mid H(\phi) < 0\} \quad (6)$$

is an inner-approximation of \mathcal{RA} .

Proof: *The avoid part : from Cond.(3) and Eq. (6), we can conclude that for any trajectory $\mathbf{x}^\phi(\cdot)$ of Eq. (1) with $\phi \in \mathcal{RA}_{in}$, the following inequality holds*

$$H(\mathbf{x}_t^\phi) \leq H(\phi) < 0 \quad \forall t \in \mathbb{R}_{\geq 0} \quad (7)$$

which is to say, the trajectories of Eq. (1) will never touch the boundary of S by Cond.(4).

The reach part : we prove that $g(\mathbf{x}^\phi(t))$ will eventually become smaller than 0 for any trajectory starting from $\phi \in \mathcal{RA}_{in}$. To the end, by using $\mathbf{x}_t^\phi(0) = \mathbf{x}^\phi(t)$, integrate both sides of Cond.(5) on t from 0 to p ($p > 0$):

$$\begin{aligned} \int_0^p g(\mathbf{x}^\phi(t))dt &\leq \int_0^p H(\mathbf{x}_t^\phi)dt - \int_0^p dw(\mathbf{x}^\phi(t)) \\ &\leq \int_0^p H(\phi)dt - \int_0^p dw(\mathbf{x}^\phi(t)) \\ &\quad \text{[by Eq. (7)]} \\ &\leq pH(\phi) - (w(\mathbf{x}^\phi(p)) - w(\phi(0))) \\ &\quad \text{[by calculating the integration]} \end{aligned}$$

Dividing both sides of the resulting inequality by p and letting p approach to infinity, then it follows

$$\begin{aligned} &\lim_{p \rightarrow \infty} \frac{\int_0^p g(\mathbf{x}^\phi(t))dt}{p} \\ &\leq H(\phi) - \lim_{p \rightarrow \infty} \frac{w(\mathbf{x}^\phi(p)) - w(\phi(0))}{p} < 0 \end{aligned}$$

where the last inequality follows because $w(\mathbf{x}^\phi(t))$ is bounded over D . Thus, there exists some $t' \in \mathbb{R}_{\geq 0}$, $g(\mathbf{x}^\phi(t')) < 0$ because of the continuity of $g(\mathbf{x})$. Hence, the trajectory must arrive at the target set T at t' . \triangleleft

Obviously, the constraints in Def. 6 are unsolvable in general. Therefore, in the next subsection, we aim to relax these constraints so that synthesizing RABFals is computable.

3.2 Inner-approximating Reach-Avoid Set

In order to efficiently inner-approximate the reach-avoid set defined in Eq. (2) using RABFals, let's consider RABFals defined in Def. 6 with the following form

$$H(\mathbf{x}_t) = h_0(\mathbf{x}_t(0)) + \int_{-\tau}^0 h_1(\mathbf{x}_t(\theta))d\theta \quad (8)$$

where $h_0(\mathbf{x}_t(0)) \in \mathbb{R}[\mathbf{x}_t(0)]$ and $h_1(\mathbf{x}_t(\theta)) \in \mathbb{R}[\mathbf{x}_t(\theta)]$.

Regarding RABFals with the form (8), we have the following theorem.

Theorem 8 *Given a DDE with domain $D \subseteq \mathbb{R}^n$, safe set S and target set T , if there exists a RABFal $H(\cdot)$ with the form (8), and a bounded function $w : D \rightarrow \mathbb{R}$, such that*

$$-\frac{\partial h_0(\mathbf{x})}{\partial \mathbf{x}} \cdot \mathbf{f}(\mathbf{x}, \mathbf{x}) - \tau \mathbf{e}_1(\mathbf{x})^T \cdot C \geq 0, \forall \mathbf{x} \in S, \quad (9)$$

$$h_0(\mathbf{x}) + \tau h_1(\mathbf{x}) + \frac{\tau^2}{2} \mathbf{e}_2(\mathbf{x})^T \cdot C \geq 0, \forall \mathbf{x} \in \partial S, \quad (10)$$

$$h_0(\mathbf{x}) + \tau h_1(\mathbf{x}) + \frac{\tau^2}{2} \mathbf{e}_2(\mathbf{x})^T \cdot C - g(\mathbf{x}) \quad (11)$$

$$-\frac{\partial w(\mathbf{x})}{\partial \mathbf{x}} \cdot \mathbf{f}(\mathbf{x}, \mathbf{x}) - \tau \mathbf{e}_3(\mathbf{x})^T \cdot C \geq 0, \forall \mathbf{x} \in S,$$

where $\mathbf{e}_1, \mathbf{e}_2, \mathbf{e}_3 \in \mathbb{R}[\mathbf{x}]^n$ and $C \in \mathbb{R}^n$ are auxiliary polynomials satisfying (the inequalities are coordinate-wise)

$$\mathbf{e}_1(\mathbf{x})^T \geq \left| \frac{\partial h_1(\mathbf{y})}{\partial \mathbf{y}} - \frac{\partial h_0(\mathbf{x})}{\partial \mathbf{x}} \cdot \frac{\partial \mathbf{f}(\mathbf{x}, \mathbf{y})}{\partial \mathbf{y}} \right|, \forall \mathbf{x}, \mathbf{y} \in S, \quad (12)$$

$$\mathbf{e}_2(\mathbf{x})^T \geq \left| \frac{\partial h_1(\mathbf{x})}{\partial \mathbf{x}} \right|, \forall \mathbf{x} \in S, \quad (13)$$

$$\mathbf{e}_3(\mathbf{x})^T \geq \left| \frac{\partial w(\mathbf{x})}{\partial \mathbf{x}} \cdot \frac{\partial \mathbf{f}(\mathbf{x}, \mathbf{y})}{\partial \mathbf{y}} \right|, \forall \mathbf{x}, \mathbf{y} \in S, \quad (14)$$

$$C \geq |\mathbf{f}(\mathbf{x}, \mathbf{y})|, \forall \mathbf{x}, \mathbf{y} \in S, \quad (15)$$

then \mathcal{RA}_{in} defined by (6) is an inner-approximation of the reach-avoid set.

The correctness of Thm. 8 follows directly from applying Thm. 7 to RABFal with the form (8) (cf. Cond. (3)–(4) and Cond. (9)–(11)). Cond. (12)–(14) are auxiliary conditions to control the extra terms during simplification.

Proof: We will show Cond. (9)–(11) imply Cond. (3)–(4) under auxiliary conditions (12)–(14), thus by Thm. 7, \mathcal{RA}_{in} is an inner-approximation of the reach-avoid set. We first present two equalities proved in [17], which rewrite the delay term $\mathbf{x}(t - \tau)$ as an integration,

$$\mathbf{f}(\mathbf{x}(t), \mathbf{x}(t - \tau)) = \mathbf{f}(\mathbf{x}(t), \mathbf{x}(t)) - \int_{t-\tau}^t \frac{\partial \mathbf{f}(\mathbf{x}(t), \mathbf{x}(\theta))}{\partial \mathbf{x}(\theta)} \cdot \dot{\mathbf{x}}(\theta) d\theta. \quad (16)$$

$$h(\mathbf{x}(t - \theta)) = h(\mathbf{x}(t)) - \int_{t-\theta}^t \frac{\partial h}{\partial \mathbf{x}} \cdot \dot{\mathbf{x}}(\rho) d\rho, \quad (17)$$

where $\theta > 0$, and $h(\cdot)$ is any differentiable function. We now show Cond. (3) holds under Cond. (9). In fact, since $H(\cdot)$ takes the form of (8), we have

$$\begin{aligned} \frac{dH(\mathbf{x}_t)}{dt} &= \frac{\partial h_0(\mathbf{x}(t))}{\partial \mathbf{x}(t)} \mathbf{f}(\mathbf{x}(t), \mathbf{x}(t)) + \int_{t-\tau}^t \left(\frac{\partial h_1(\mathbf{x}(\theta))}{\partial \mathbf{x}(\theta)} - \frac{\partial h_0(\mathbf{x}(t))}{\partial \mathbf{x}(t)} \cdot \frac{\partial \mathbf{f}(\mathbf{x}(t), \mathbf{x}(\theta))}{\partial \mathbf{x}(\theta)} \right) \cdot \dot{\mathbf{x}}(\theta) d\theta \\ &\leq \frac{\partial h_0(\mathbf{x}(t))}{\partial \mathbf{x}(t)} \mathbf{f}(\mathbf{x}(t), \mathbf{x}(t)) + \int_{t-\tau}^t \left| \frac{\partial h_1(\mathbf{x}(\theta))}{\partial \mathbf{x}(\theta)} - \frac{\partial h_0(\mathbf{x}(t))}{\partial \mathbf{x}(t)} \cdot \frac{\partial \mathbf{f}(\mathbf{x}(t), \mathbf{x}(\theta))}{\partial \mathbf{x}(\theta)} \right| \cdot |\dot{\mathbf{x}}(\theta)| d\theta \\ &\leq \frac{\partial h_0}{\partial \mathbf{x}(t)} \mathbf{f}(\mathbf{x}(t), \mathbf{x}(t)) + \mathbf{e}_1(\mathbf{x}(t))^T \cdot \tau C \\ &\leq 0. \end{aligned} \quad \begin{array}{l} \text{[by Eq. (16)]} \\ \text{[by auxiliary conditions (12), (15)]} \\ \text{[by Cond. (9)]} \end{array}$$

This proves Cond. (3). Then we prove Cond. (4) holds under Cond. (10). Since $H(\cdot)$ takes the form (8), we have

$$\begin{aligned} H(\mathbf{x}_t) &= h_0(\mathbf{x}(t)) + \int_{-\tau}^0 \left(h_1(\mathbf{x}(t)) - \int_{t+\theta}^t \frac{\partial h_1(\mathbf{x}(\rho))}{\partial \mathbf{x}(\rho)} \cdot \dot{\mathbf{x}}(\rho) d\rho \right) d\theta \\ &= h_0(\mathbf{x}(t)) + \tau h_1(\mathbf{x}(t)) - \int_{-\tau}^0 \int_{t+\theta}^t \frac{\partial h_1(\mathbf{x}(\rho))}{\partial \mathbf{x}(\rho)} \cdot \dot{\mathbf{x}}(\rho) d\rho d\theta \\ &\geq h_0(\mathbf{x}(t)) + \tau h_1(\mathbf{x}(t)) - \int_{-\tau}^0 \int_{t+\theta}^t \left| \frac{\partial h_1(\mathbf{x}(\rho))}{\partial \mathbf{x}(\rho)} \right| \cdot |\dot{\mathbf{x}}(\rho)| d\rho d\theta \\ &\geq h_0(\mathbf{x}(t)) + \tau h_1(\mathbf{x}(t)) - \int_{-\tau}^0 \int_{t+\theta}^t \mathbf{e}_2(\mathbf{x}(t))^T \cdot C d\rho d\theta \\ &= h_0(\mathbf{x}(t)) + \tau h_1(\mathbf{x}(t)) + \frac{\tau^2}{2} \mathbf{e}_2(\mathbf{x}(t))^T \cdot C \\ &\geq 0, \end{aligned} \quad \begin{array}{l} \text{[by Eq. (16)]} \\ \text{[by auxiliary conditions (13), (15)]} \\ \text{[by Cond. (10)]} \end{array}$$

thus Cond. (4) holds.

Finally, we show Cond. (5) holds under Cond. (11). In fact,

$$\begin{aligned} H(\mathbf{x}_t) - g(\mathbf{x}_t(0)) &- \frac{dw(\mathbf{x}_t(0))}{dt} \\ &= h_0(\mathbf{x}(t)) + \tau h_1(\mathbf{x}(t)) - \int_{-\tau}^0 \int_{t+\theta}^t \frac{\partial h_1(\mathbf{x}(\rho))}{\partial \mathbf{x}(\rho)} \cdot \dot{\mathbf{x}}(\rho) d\rho d\theta - \\ &g(\mathbf{x}(t)) - \frac{\partial w(\mathbf{x}(t))}{\partial \mathbf{x}(t)} \cdot \mathbf{f}(\mathbf{x}(t), \mathbf{x}(t)) + \\ &\int_{t-\tau}^t \frac{\partial w(\mathbf{x}(t))}{\partial \mathbf{x}(t)} \cdot \frac{\mathbf{f}(\mathbf{x}(t), \mathbf{x}(\theta))}{\mathbf{x}(\theta)} \cdot \dot{\mathbf{x}}(\theta) d\theta \\ &\geq h_0(\mathbf{x}(t)) + \tau h_1(\mathbf{x}(t)) + \frac{\tau^2}{2} \mathbf{e}_2(\mathbf{x}(t))^T \cdot C - g(\mathbf{x}(t)) - \\ &\frac{\partial w}{\partial \mathbf{x}(t)} \mathbf{f}(\mathbf{x}(t), \mathbf{x}(t)) - \int_{t-\tau}^t \mathbf{e}_3(\mathbf{x}(t)) \cdot C d\theta \\ &= h_0(\mathbf{x}(t)) + \tau h_1(\mathbf{x}(t)) + \frac{\tau^2}{2} \mathbf{e}_2(\mathbf{x}(t))^T \cdot C - g(\mathbf{x}(t)) - \\ &\frac{\partial w}{\partial \mathbf{x}(t)} \mathbf{f}(\mathbf{x}(t), \mathbf{x}(t)) - \tau \mathbf{e}_3(\mathbf{x}(t)) \cdot C \\ &\geq 0, \end{aligned} \quad \begin{array}{l} \text{[by Eq. (16) and (17)]} \\ \text{[by auxiliary conditions (13), (14), (15)]} \\ \text{[by Cond. (11)]} \end{array}$$

thus Cond. (5) holds. This completes the proof. \triangleleft

All constraints in Thm. 8 can be encoded as a SDP problem. Thus, when S and T are semialgebraic, we can exploit SDP solving [28] to synthesize RABFal $H(\mathbf{x}_t)$ of the form (8) in a standard way, which is implemented by Algorithm Alg. 1 below.

Alg. 1 predefines polynomial templates for $H(\mathbf{x}_t)$ with degree `deg` first, and then utilizes an SOS solver to find a RABFal by solving the resulting SDP problem. If a RABFal is synthesized, then the procedure terminates, otherwise repeat the above procedure by trying another polynomial templates with higher degree, until the degree of polynomial templates reach to the threshold `MaxDeg`.

Remark 3 For simplification of exposition, in Alg. 1, S and T are defined by a single polynomial. But it can be easily extended to general semialgebraic sets without any substantial change, only by adding additional Lagrangian multiplier polynomials $l(\mathbf{x}(t)) \in \Sigma[\mathbf{x}(t)]$.

Remark 4 The objective function of the optimization problem in Alg. 1 is set to be the summation of the coefficients of $\mathbf{e}_1, \mathbf{e}_2, \mathbf{e}_3$. This helps to ensure that the estimations of the absolute values are as accurate as possible.

Example 9 Let us continue Example 2. Consider the DDE defined by the vector field in mode q_1 , that is

$$\begin{aligned} \dot{x}_1(t) &= 0.5x_2(t) + 0.5x_2(t - 0.1) \\ \dot{x}_2(t) &= -0.5x_1(t) - 0.5x_1(t - 0.1) - 1.5x_2(t) \end{aligned}$$

which is same as [37]. In order to ease the comparison with [37], we simply set h_1 in Eq. (8) to 0 in this example.

Algorithm 1 InRA (\mathbf{f}, S, T)

Require: A polynomial vector field $\mathbf{f}(\mathbf{x}(t), \mathbf{x}(t - \tau))$, a safe set $S = \{\mathbf{x} \in \mathbb{R}^n \mid s(\mathbf{x}) \leq 0\}$ and a target set $T = \{\mathbf{x} \in \mathbb{R}^n \mid g(\mathbf{x}) \leq 0\}$

Ensure: A synthesize RABFal $H(\mathbf{x}_t)$ whose 0-sublevel set is an inner-approximation of the reach-avoid set

- 1: $\text{deg} \leftarrow 1$
- 2: **repeat**
- 3: Predefine polynomial template h_0, h_1 with degree deg
- 4: Predefine polynomial template e_1, e_2, e_3 with degree deg
- 5: Predefine enough Lagrangian polynomials l_i with degree deg
- 6: Approximate the upper bound of \mathbf{f} over domain D and assign the bound to C
- 7: Solve the following SOS optimization problem:

$$\begin{aligned} \min \quad & \text{the sum of the coefficient of } e_1, e_2, e_3 \\ \text{s.t.} \quad & \left\{ \begin{array}{l} -\frac{\partial h_0}{\partial \mathbf{x}} \cdot \mathbf{f}(\mathbf{x}, \mathbf{x}) - \tau e_1(\mathbf{x})^T \cdot C + l_1(\mathbf{x})s(\mathbf{x}) \in \Sigma[\mathbf{x}], \quad l_1 \in \Sigma[\mathbf{x}] \\ h_0(\mathbf{x}) + \tau h_1(\mathbf{x}) + \frac{\tau^2}{2} e_2(\mathbf{x})^T \cdot C + l_0(\mathbf{x})s(\mathbf{x}) \in \Sigma[\mathbf{x}], \\ h_0(\mathbf{x}) + \tau h_1(\mathbf{x}) + \frac{\tau^2}{2} e_2(\mathbf{x})^T \cdot C - g(\mathbf{x}) - \frac{\partial w}{\partial \mathbf{x}} \cdot \mathbf{f}(\mathbf{x}, \mathbf{x}) - \tau e_3(\mathbf{x})^T \cdot C + l_2(\mathbf{x})s(\mathbf{x}) \in \Sigma[\mathbf{x}], \quad l_2 \in \Sigma[\mathbf{x}] \\ e_1(\mathbf{x}) - \left(\frac{\partial h_1(\mathbf{y})}{\partial \mathbf{y}} - \frac{\partial h_0(\mathbf{x})}{\partial \mathbf{x}} \cdot \frac{\partial \mathbf{f}(\mathbf{x}, \mathbf{y})}{\partial \mathbf{y}} \right) + l_3(\mathbf{x}, \mathbf{y})s(\mathbf{x}) + l_4(\mathbf{x}, \mathbf{y})s(\mathbf{y}) \in \Sigma[\mathbf{x}, \mathbf{y}]^n, \quad l_3, l_4 \in \Sigma[\mathbf{x}, \mathbf{y}]^n \\ e_1(\mathbf{x}) + \left(\frac{\partial h_1(\mathbf{y})}{\partial \mathbf{y}} - \frac{\partial h_0(\mathbf{x})}{\partial \mathbf{x}} \cdot \frac{\partial \mathbf{f}(\mathbf{x}, \mathbf{y})}{\partial \mathbf{y}} \right) + l_5(\mathbf{x}, \mathbf{y})s(\mathbf{x}) + l_6(\mathbf{x}, \mathbf{y})s(\mathbf{y}) \in \Sigma[\mathbf{x}, \mathbf{y}]^n, \quad l_5, l_6 \in \Sigma[\mathbf{x}, \mathbf{y}]^n \\ e_2(\mathbf{x}) - \frac{\partial h_1(\mathbf{x})}{\partial \mathbf{x}} + l_7(\mathbf{x})s(\mathbf{x}) \in \Sigma[\mathbf{x}]^n, \quad e_2(\mathbf{x}) + \frac{\partial h_1(\mathbf{x})}{\partial \mathbf{x}} + l_8(\mathbf{x})s(\mathbf{x}) \in \Sigma[\mathbf{x}]^n, \quad l_7, l_8 \in \Sigma[\mathbf{x}]^n \\ e_3(\mathbf{x}) - \frac{\partial w(\mathbf{x})}{\partial \mathbf{x}} \cdot \frac{\partial \mathbf{f}(\mathbf{x}, \mathbf{y})}{\partial \mathbf{y}} + l_9(\mathbf{x}, \mathbf{y})s(\mathbf{x}) + l_{10}(\mathbf{x}, \mathbf{y})s(\mathbf{y}) \in \Sigma[\mathbf{x}, \mathbf{y}]^n, \quad l_9, l_{10} \in \Sigma[\mathbf{x}, \mathbf{y}]^n \\ e_3(\mathbf{x}) + \frac{\partial w(\mathbf{x})}{\partial \mathbf{x}} \cdot \frac{\partial \mathbf{f}(\mathbf{x}, \mathbf{y})}{\partial \mathbf{y}} + l_{11}(\mathbf{x}, \mathbf{y})s(\mathbf{x}) + l_{12}(\mathbf{x}, \mathbf{y})s(\mathbf{y}) \in \Sigma[\mathbf{x}, \mathbf{y}]^n, \quad l_{11}, l_{12} \in \Sigma[\mathbf{x}, \mathbf{y}]^n \\ e_i(\mathbf{x}) \in \Sigma[\mathbf{x}]^n, \quad i = 1, 2, 3. \end{array} \right. \end{aligned}$$

- 8: **if** the optimization problem above is solved successfully **then**
 - 9: **return** $H(\mathbf{x}_t) = h_0(\mathbf{x}_t(0)) + \int_{-\tau}^0 h_1(\mathbf{x}_t(\theta)) d\theta$
 - 10: **end if**
 - 11: $\text{deg} \leftarrow \text{deg} + 1$
 - 12: **until** $\text{deg} = \text{MaxDeg}$
-

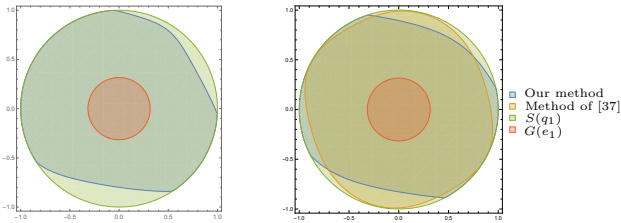


Fig. 3. Comparison between the method in [37] and ours

The right side of Fig. 3 shows the reach-avoid set of mode q_1 , with $G(e_1)$ as the target (depicted in red) and $\{(x_1, x_2) \mid x_1^2 + x_2^2 - 1 \leq 0\}$ as safe set (depicted in green). Clearly, Alg. 1 gives a more conservative reach-avoid set (depicted in blue) compared to the method in [37] (depicted in orange). On the left side of Fig. 3, we modify the vector field of q_1 by changing the delay from 0.1 to 0.3,

that is not solvable with [37]'s method. while Alg. 1 can still efficiently compute a result (depicted in blue). \triangleleft

4 Constructing Discrete Directed Graph

In this section, we introduce the second step of our approach, that is, to construct a discrete directed graph from the considered dHA \mathcal{H} based on the computed reach-avoid sets for all its modes.

4.1 Mode Partition

To avoid the difficulty caused by non-determinism in the third step of reset controller synthesis, the constructed discrete directed graph from \mathcal{H} should be deterministic. So, in this subsection, by employing Alg. 1, we will give a mode partition algorithm to split a single mode of dHA into some sub-modes, such that for any two of these sub-modes the reach-avoid sets of their guard conditions and target sets are disjoint. Moreover, such partition will

help us to abstract away the continuous part of dHA and transform it into a discrete directed graph, which in turn simplifies the process of synthesizing reset maps (as will be discussed in Section 5).

We firstly employ the running example to give an intuitive explanation of our partition algorithm.

Example 10 Consider Example 2, where the safe set defined as $S_{q_1} = S_{q_2} = S_{q_3} = \{(x_1, x_2) \mid x_1^2 + x_2^2 - 1 \leq 0\}$, the target set is $T_{q_3} = \{(x_1, x_2) \mid x_1^2 + x_2^2 \leq 0.1\}$ and $T_{q_1} = T_{q_2} = \emptyset$. The procedure of mode partition for q_1 is illustrated in Fig. 4. We denote the reach-avoid set computed by Alg. 1 in mode q_i as $\mathcal{RA}_{in}(i, j)$, where g_{ij} represents the target (as defined in Fig. 4). Therefore, the regions enclosed by the green, red, and purple curves in mode q_1 (as shown in Fig. 4) can be described as follows:

$$\begin{aligned} \mathcal{RA}_{in}(1, 1) &:= \text{InRA}(f_1, \text{Dom}(q_1) \cap S_{q_1}, g_{11} \setminus \text{Dom}(q_1)), \\ \mathcal{RA}_{in}(1, 2) &:= \text{InRA}(f_1, \text{Dom}(q_1) \cap S_{q_1}, g_{12} \setminus \text{Dom}(q_1)), \\ \mathcal{RA}_{in}(1, 3) &:= \text{InRA}(f_1, \text{Dom}(q_1) \cap S_{q_1}, g_{13} \setminus \text{Dom}(q_1)). \end{aligned}$$

Please note that, strictly speaking, $\mathcal{RA}_{in}(\cdot)$ represents a set of functions and should not be depicted in the same figure with $\text{Dom}(q_1) \in \mathbb{R}^2$. However, for the purpose of providing an intuitive perspective, we included these sets together.

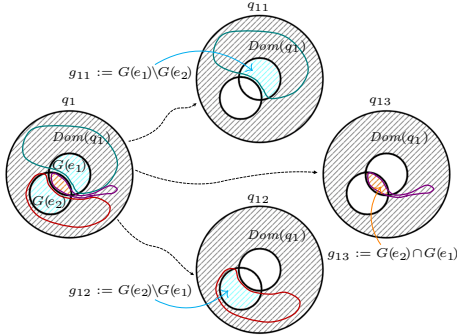


Fig. 4. Mode partition of q_1 . On the left side, we have mode q_1 with guard conditions $G(e_1)$ and $G(e_2)$ represented by blue slashes, and their intersection depicted by orange slashes. The reach-avoid set to $G(e_1) \cup G(e_2)$ can be partitioned into three disjoint regions: g_{11} , g_{12} , and g_{13} , as shown above. Accordingly, mode q_1 is partitioned into three sub-modes: q_{11} , q_{12} , and q_{13} .

The partition of q_3 is illustrated in Fig. 5. We denote the regions enclosed by the green and blue curves, computed using Alg. 1 with g_{30} and g_{31} as the respective targets, as $\mathcal{RA}_{in}(3, 0)$ and $\mathcal{RA}_{in}(3, 1)$.

After partitioning all modes, new edges should be introduced. Let's consider q_{31} , edges from q_{31} to the sub-modes of q_1 are introduced, i.e., including (q_{31}, q_{11}) , (q_{31}, q_{12}) , and (q_{31}, q_{13}) . Accordingly, the reset maps associated with them are given as:

- $R^m((q_{31}, q_{11}), G^m(q_{31}, q_{11})) = \mathcal{RA}_{in}(1, 1)$,
- $R^m((q_{31}, q_{12}), G^m(q_{31}, q_{12})) = \mathcal{RA}_{in}(1, 2)$,
- $R^m((q_{31}, q_{13}), G^m(q_{31}, q_{13})) = \mathcal{RA}_{in}(1, 3)$.

where $G^m(q_{31}, q_{11}) = G^m(q_{31}, q_{12}) = G^m(q_{31}, q_{13}) = g_{31}$.

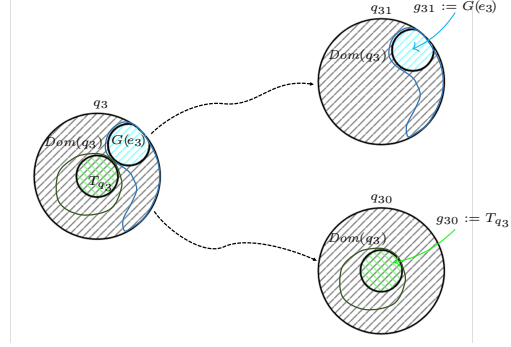


Fig. 5. Mode partition of q_3 . The left side is mode q_3 with the guard condition $G(e_3)$ (blue slashes) and the target set T_{q_3} (green slashes). Correspondingly, q_3 is partitioned into two sub-modes: q_{30} with $g_{30} = T_{q_3}$, and q_{31} with $g_{31} = G(e_3)$.

Similarly, for q_{13} , edges from q_{13} to the sub-modes of q_2 and q_3 should be introduced, whose reset map can be defined in the same way. \triangleleft

Remark 5 Note that we set the third input of $\text{InRA}(\cdot, \cdot, \cdot)$ in $\mathcal{RA}_{in}(1, 1)$ to $g_{11} \setminus \text{Dom}(q_1)$ rather than g_{11} simply in order to remove non-determinism between continuous evolution and discrete transition. As an execution remains in $g_{11} \cap \text{Dom}(q_1)$, it can either take the discrete transition immediately, or continue the continuous evolution. However, whenever it reaches to $g_{11} \cap \neg \text{Dom}(q_1)$, the discrete jump has to happen.

We present the mode partition algorithm in Alg. 2. The algorithm proceeds as follows: Firstly, it iteratively partitions all modes of \mathcal{H} (line 1 to line 15). During each iteration, a sub-mode is added if the reach-avoid set to the target set is non-empty (line 2 to line 5). Next, the guard conditions are partitioned so that the corresponding reach-avoid sets are disjoint (line 6). Based on the resulting partition, each mode is also partitioned into sub-modes accordingly (line 8 to line 14). Finally, we introduce edges to \mathcal{H}^m in accordance with \mathcal{H} and synthesize a reset map accordingly (line 16 to line 25). The correctness of Alg. 2 is guaranteed by Thm. 8.

4.2 Transforming to Discrete Directed Graph

For a given dHA $\mathcal{H} = (Q, X, \text{Dom}, F, \text{Init}, E, G, ST, R)$, let $\mathcal{H}^m = (Q^m, X, \text{Dom}^m, F^m, \text{Init}^m, E^m, G^m, ST^m, R^m)$ be the resulting dHA after applying Alg. 2 to \mathcal{H} . Thus, a discrete directed graph $\text{DG} = (V, E, V_0, V_T)$ can be defined as follows:

- $V = Q^m$ is the set of vertices;
 - $E = E^m$ is the set of directed edges (arcs);
 - $V_0 = \{q \in Q^m \mid \text{Init}^m(q) \neq \emptyset\}$ is the set of initial vertices;
 - $V_T = \{q \in Q^m \mid T_q^m \neq \emptyset\}$ is the set of target vertices.
- Note that our definition above slightly differs from the standard definition of directed graph by allowing V_0 and V_T .

The following running example illustrates the above transformation.

Example 11 Let's continue the dHA given in Example 2 (see Fig. 2). In Example 10, q_2 is partitioned into three

Algorithm 2 ModePartition(\mathcal{H}, S, T)

Require: A dHA $\mathcal{H} = (Q, X, Dom, F, Init, E, G, ST, R)$,
a safe set $S \subseteq Q \times X$, a target set $T \subseteq Q \times X$

Ensure: The dHA $\mathcal{H}^m = (Q^m, X, Dom^m, F^m, Init^m, E^m, G^m, ST^m, R^m)$ and target set T^m , safe set S^m after partition

/ Partition modes of \mathcal{H} into sub-modes based on the result of reach-avoid analysis */*

```

1: for  $q_i \in Q$  do
2:    $\mathcal{RA}_{in}(i, 0) \leftarrow \text{InRA}(\mathbf{f}_i, \text{Dom}(q_i) \cap S_{q_i}, T_{q_i})$ 
3:   if  $\mathcal{RA}_{in}(i, 0)$  is not empty then
4:     Add  $q_{i0}$  to  $Q^m$ , with  $\text{Dom}^m(q_{i0}) = \text{Dom}(q_i)$ ,
        $\mathbf{f}_{i0}^m = \mathbf{f}_i$ ,  $\text{Init}^m(q_{i0}) = \text{Init}(q_i) \cap \mathcal{RA}_{in}(i, 0)$ ,
        $T_{q_{i0}}^m = T_{q_i}$ ,  $S_{q_{i0}}^m = S_{q_i}$ 
5:   end if
6:   Partition the guard conditions of edges jumping
   from  $q_i$  into disjoint sets, and store these sets in  $G_i$ 
7:    $j \leftarrow 1$ 
8:   for  $g_{ij} \in G_i$  do
9:      $\mathcal{RA}_{in}(i, j) \leftarrow \text{InRA}(\mathbf{f}_i, \text{Dom}(q_i) \cap S_{q_i}, g_{ij} \setminus \text{Dom}(q_i))$ 
10:    if  $\mathcal{RA}_{in}(i, j)$  is not empty then
11:      Add  $q_{ij}$  to  $Q^m$ , with  $\text{Dom}^m(q_{ij}) = \text{Dom}(q_i)$ ,
         $\mathbf{f}_{ij}^m = \mathbf{f}_i$ ,  $\text{Init}^m(q_{ij}) = \text{Init}(q_i) \cap \mathcal{RA}_{in}(i, j)$ ,
         $T_{q_{ij}}^m = \emptyset$ ,  $S_{q_{ij}}^m = S_{q_i}$ 

```

```

12:   end if
13:    $j \leftarrow j + 1$ 
14:   end for
15:   end for
   /* Rebuild the edges of  $\mathcal{H}^m$  */
16:   for  $q_i \in Q$  do
17:     for each sub-mode  $q_{ij}$  of  $q_i$  with guard condition
        $g_{ij}$  in it do
18:        $\text{Post}(q_{ij}) \leftarrow \{p \in Q \mid g_{ij} \subseteq G(q_i, p)\}$ 
       /*  $\text{Post}(q_{ij})$  contains the modes in  $\mathcal{H}$  such that
          $g_{ij}$  is the intersection of guard conditions of
         edges from  $q_i$  to these modes */
19:       for  $q_j \in \text{Post}(q_{ij})$  do
20:         for each sub-mode  $q_{jk}$  of  $q_j$  do
21:           Add edge  $e = (q_{ij}, q_{jk})$  to  $E^m$ , with
              $G^m(e) = g_{ij}$ ,  $R^m(e, G^m(e)) = \mathcal{RA}_{in}(j, k)$ 
22:         end for
23:       end for
24:     end for
25:   end for
26:    $\mathcal{H}^m = (Q^m, X, \text{Dom}^m, F^m, \text{Init}^m, E^m, G^m, ST^m, R^m)$ 
27:   return  $\mathcal{H}^m, T^m, S^m$ 

```

sub-modes, q_3 is partitioned into two sub-modes, while q_2 does not need to be partitioned. The resulting discrete directed graph is depicted in Fig. 6, where $V_0 = \{q_{11}, q_{12}, q_{13}\}$ and $V_T = \{q_{30}\}$. \triangleleft

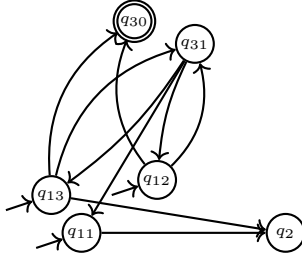


Fig. 6. The resulting discrete directed graph

5 Reset Controller Synthesis

In this section, we focus on the third step of our approach, which involves synthesizing a reset controller for a given dHA \mathcal{H} utilizing the discrete directed graph obtained from \mathcal{H} in the second step.

5.1 Pruning the Resulting Discrete Directed Graph

In this subsection, we will present a method to prune some edges that may violate the reach-avoid property from the discrete directed graph derived in the second step by redefining their reset maps.

As shown in Fig. 6 in Example 11, there are two types of scenarios that may violate the reach-avoid property:

Algorithm 3 PruningNonTargetSink(DG)

Require: $\text{DG} = \{V, A, V_0, V_T\}$

Ensure: $\text{DG}' = \{V', A', V'_0, V'_T\}$ without non-target sinks

```

1:  $V' \leftarrow V, A' \leftarrow A, V'_0 \leftarrow V_0$ 
2:  $u \leftarrow$  the number of modes in  $V$ 
3: construct the adjacent matrix  $M = (m_{ij})_{u \times u}$  for DG
4: repeat
5:    $S \leftarrow \{q_s \notin V_T \mid \sum_{i=1}^u m_{si} = 0\}$ , flag  $\leftarrow 0$ 
6:   for  $q_s \in S$  do
7:     for  $i = 1$  to  $u$  do
8:       if  $(q_i, q_s) \in A$  then  $A' \leftarrow A \setminus \{(q_i, q_s)\}$ ,
9:          $m_{is} \leftarrow 0$ , flag  $\leftarrow 1$ 
10:    end for
11:    $V' \leftarrow V' \setminus \{q_u\}, V'_0 \leftarrow V'_0 \setminus \{q_u\}$ 
12:   end for
13: until flag=0
14: return  $\text{DG}' = \{V', A', V'_0, V'_T\}$ 

```

1. The first case is “non-target sink”. A sink refers to a vertex with no outgoing edges. This occurs when a path terminates at a sink that does not belong to V_T . An example is the path $\langle q_{11}, q_2 \rangle$ in Fig. 6, which terminates at q_2 with $q_2 \notin V_T$. To address this issue, our pruning algorithm will iteratively remove all non-target sinks and their incoming arcs until none non-target sinks are left. (Alg. 3). For instance, Alg. 3 will prune (q_{11}, q_2) , (q_{13}, q_2) , (q_{31}, q_{11}) and (q_{31}, q_{13}) in Fig. 6.
2. The second type is referred to as “simple loop”. This

occurs when the discrete directed graph contains a simple loop, in which at most one vertex can appear twice, such as $\langle q_{12}, q_{31}, q_{12} \rangle$ in Fig. 6. Clearly, such path could be executed infinitely. So it is impossible to reach any target in case no target vertex is contained in the loop. To address this issue, we propose another algorithm (Alg. 4) to break simple loop by removing some edges on the path backwards. For instance, in Fig. 6, we prune (q_{12}, q_{31}) and (q_{31}, q_{12}) in order to break the simple loop $\langle q_{12}, q_{31}, q_{12} \rangle$.

Alg. 3 iteratively removes non-target sinks and their incoming arcs. With the aid of adjacent matrix given by line 4, such vertex $q_s \notin V_T$ can be detected if $\sum_{i=1}^u m_{si} = 0$ (line 6). Next, Alg. 3 removes all transitions to it, and in case new vertices without incoming transitions are created in the removal process, we conduct this part iteratively until no non-target sinks left.

Alg. 4 is to address the two previously mentioned cases by blocking simple loops that do not reach the target set and pruning non-target sinks. To begin with, the algorithm iteratively identifies simple loops within DG' , and removes a selected edge from each loop (line 4). This process continues until there are no more simple loops present in DG' . Subsequently, Alg. 4 is applied to prune all non-target sinks within the resulting modified discrete directed graph (line 6). Finally, the algorithm returns the modified discrete directed graph as the output (line 7).

Algorithm 4 PruningGraph(DG)

Require: $DG = \{V, A, V_0, V_T\}$

Ensure: $DG' = \{V', A', V'_0, V'_T\}$ satisfying the reach-avoid constraints

- 1: $V' \leftarrow V, A' \leftarrow A, V'_0 \leftarrow V_0, V'_T \leftarrow V_T$
 - 2: **repeat**
 - 3: Find a simple loop c in DG'
 - 4: $A' \leftarrow A' \setminus e$, where $e = (p, q) \in A'$ is an edge in c
 - 5: **until** There is no simple loop in DG'
 - 6: $DG' \leftarrow \text{PruningNonTargetSink}(DG')$
 - 7: **return** $DG' = \{V', A', V'_0, V'_T\}$
-

5.2 Reset Controller Synthesis from Discrete Directed Graph

In this subsection, our focus is on synthesizing a reset controller based on the resulting discrete directed graph DG' obtained from applying Alg. 3 and Alg. 4. The goal is to generate a reset map associated with each edge in the original dHA \mathcal{H} . This is achieved by merging the reset maps derived from the mode partitioned dHA \mathcal{H}^m using Alg. 2, and then refining the initial set and restricting the reset map according to the structure of DG' .

Let's continue the running example to illustrate the basic idea in the following.

Example 12 *By applying Alg. 4 to Example 11, the resulting discrete directed graph DG' is presented in Fig. 7. In the following, we will use $R^m(\cdot)$ and $\text{Init}^m(\cdot)$ to represent the resulting reset map and initial set from the running example by applying Alg. 2.*

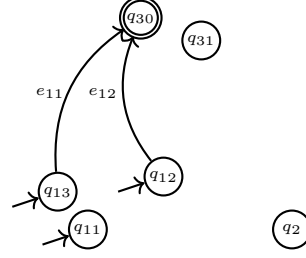


Fig. 7. The discrete directed graph of Example 11 after applying Alg. 4

- $R^r(e_2, G(e_2) \setminus G(e_1))^2 = R^m(e_{12}, G^m(e_{12}))$, corresponding to e_{12} in Fig. 7;
- $R^r(e_2, G(e_2) \cap G(e_1)) = R^m(e_{11}, G^m(e_{11}))$, corresponding to e_{32} in Fig. 7;
- $\text{Init}^r(q_1) = \text{Init}^m(q_{13}) \cup \text{Init}^m(q_{14})$, corresponding to e_{11} and e_{12} in Fig. 7;
- R^r will associate null map with other edges and Init^r assigns initial sets in other mode to be empty.

Thus, with the re-defined reset map and initial set, all executions of dHA in Example 2 will reach to the target set within q_2 , while ensuring safety before the reaching. \triangleleft

We implement all above ideas together in Alg. 5. Line 1 applies Alg. 2 to obtain a deterministic dHA \mathcal{H}^m . Line 2 obtains a discrete directed graph DG from \mathcal{H}^m . Then, line 3 prunes all simple loops and non-target sinks that cannot reach the target set using Alg. 4. Afterwards, Alg. 5 tries to redefine a reset map and refine the initial set by traversing all modes of \mathcal{H} (line 4 to line 16). In each iteration, the initial set of the selected mode q_i is set to be empty first (line 5); for each sub-mode q_{ij} of q_i , P collects all submodes q_{kl} from DG' , where there is an edge between q_i and q_k in \mathcal{H} , and then the reset map associated with (q_i, q_k) is set to be the union of all reset maps associated with (p_{ij}, p) in DG' , where $p \in P$; correspondingly, the initial set of q_i is set to the union of the initial set of q_{ij} , where q_{ij} in DG' is a submode of p_i .

Theorem 13 (Correctness) *Problem 1 is solvable if and only if the Init^r obtained from Alg. 5 is non-empty.*

- **Termination:** Alg. 5 terminates in finite steps;
- **Soundness:** Any reset controller synthesized by Alg. 5 does solve Problem 1;
- **Completeness:** If Problem 1 can be solved by a reset controller, Alg. 5 does synthesize one.

Proof: (Termination): As the **for-loops** in Alg. 5 are finite, Alg. 5 terminates if Alg. 2 and Alg. 4 terminates. Since any component in dHA \mathcal{H} is finite, the termination of Alg. 2 follows directly. For Alg. 4, as the number of edges and vertices decrease at least one in each iteration, the “pruning” process will finally terminates, thus Alg. 4 terminates for any discrete directed graphs. This proves the termination of Alg. 5.

(Soundness): We will show any reset controller synthesized by Alg. 4 drives the modified dHA \mathcal{H}^r into target

² the e_1, e_2 here is the edge of dHA labeled in Fig. 2

Algorithm 5 Reset Control Synthesis for dHA

Require: A dHA $\mathcal{H} = (Q, X, Dom, F, Init, E, G, ST, R)$, safe set $S \subseteq Q \times X$, and target set $T \subseteq Q \times X$

Ensure: $\mathcal{H}^r = (Q, X, Dom, F, Init^r, E, G, ST, R^r)$ satisfying the safety together with the liveness constraints.

- 1: $\mathcal{H}^m, T^m, S^m \leftarrow \text{ModePartition}(\mathcal{H}, S, T)$
- 2: $\text{DG} \leftarrow \{V, A, V_0, V_T\}$
- 3: $\text{DG}' = \{V', A', V'_0, V'_T\} \leftarrow \text{PruningGraph}(\text{DG})$
- 4: **for** $q_i \in Q$ of \mathcal{H} **do**
- 5: $Init^r(q_i) \leftarrow \emptyset$
- 6: **for** each sub-mode q_{ij} of q_i **do**
- 7: $Post(q_{ij}) \leftarrow \{q_k \in Q \mid (q_{ij}, q_{kl}) \in A' \text{ with } q_{kl} \in V' \text{ being a sub-mode of } q_k\}$
- 8: **for** $q_k \in Post(q_{ij})$ **do**
- 9: $P \leftarrow \{q_{kl} \mid q_{kl} \text{ is a sub-mode of } q_k \text{ and } (q_{ij}, p_{kl}) \in A'\}$
 /* P contains any sub-mode of q_k which has an edge from q_{ij} and is not pruned in Alg. 4 */
- 10: $R^r((q_i, q_k), G^m(q_{ij}, q_{kl})) \leftarrow \bigcup_{p \in P} R^m((q_{ij}, p), G(q_{ij}, p))$
- 11: **end for**
- 12: **if** $Post(q_{ij}) \neq \emptyset$ **then**
- 13: $Init^r(q_i) \leftarrow Init^r(q_i) \cup Init^m(q_{ij})$
- 14: **end if**
- 15: **end for**
- 16: **end for**
- 17: **if** $Init^r \neq \emptyset$ **then**
- 18: **return** $\mathcal{H}^r = (Q, X, Dom, F, Init^r, E, G, ST, R^r)$
- 19: **else return** "Synthesis fail"
- 20: **end if**

set while avoiding unsafe set. To this end, we first show Alg. 4 ensures liveness.

Observation: Suppose $\text{DG}' = \text{PruningGraph}(\text{DG})$ is the output discrete directed graph of Alg. 4, then DG' will eventually visit target vertices from any initial vertex.

Justification: Note after removing all simple loops in Alg. 4 (line 2-4), any path is a finite path. Suppose $v_0 v_1 \dots v_t$ is a finite path of DG' , such that $v_0 \in V_0$, and v_t has no successor. We only need to show $v_t \in V_t$, which implies the finite path visit target vertices. In fact, line 6 in Alg. 4 ensures v_t is a target vertex, since Alg. 3 iteratively removes all non-target vertex which dose not have successor (cf. line 4-12).

We now show the synthesized dHA \mathcal{H}^r will drive the system into target while staying in safe. Let $\langle (I_0, q_0, \mathbf{x}(t)), (I_1, q_1, \mathbf{x}(t)), \dots, (I_i, q_i, \mathbf{x}(t)), \dots \rangle$ denote a hybrid execution of \mathcal{H}^r . For safety, since all reset maps are set to be the reach-avoid set (cf. Alg. 2 and Alg. 5), the trajectory is ensured to be safe (cf. Alg. 8). For liveness, since all sub-mode q_{ij} are merge into mode q_i (cf. Alg. 5 line 4-16), the above observation implies the trajectory will finally enter target mode, thus entering target set (as the reset map is set to reach target set in Alg. 2). This proves the soundness of Alg. 5.

(Completeness): We will show if there exists a reset controller that drives the system into target while staying

in safe, then Alg. 5 will output a reset controller that solves Problem 1.

Proof by contradiction. Suppose Alg. 5 reports no feasible reset controller, while there exists a reset controller that drives the modified system \mathcal{H}^r into target while staying in safe. By construction of the discrete directed graph, \mathcal{H}^r is the one corresponding to a discrete directed graph DG^r , such that DG^r eventually enter target vertices. Clearly DG^r does not contain any "non-target sinks" or "simple loops", otherwise we can find a path that does not enter target vertices. However, Alg. 4³ and Alg. 3 effectiveness remove all simple loops and non-target sinks and reports an empty discrete directed graph, this contradicts to the existence of DG^r . This complete the proof.

6 Implementation and Experiments

To further illustrate the efficacy of our approach, we implement a prototypical tool using MATLAB (2022b) and Python. Alg. 2 is implemented in MATLAB (2022b), integrated with YALMIP [25] and MOSEK [4] to formulate and solve the underlying SOS constraints. Alg. 3 and Alg. 4 are implemented in Python, leveraging the NetworkX package to manipulate the resulted discrete directed graph.

We first apply the tool to a nonlinear system of prey-predator, and subsequently evaluate its performance on a collection of benchmark examples⁴ in the literature to demonstrate the scalability of our approach. All experiments are conducted on an Apple M2 laptop with 8GB of RAM, operating on macOS Ventura (V13.2). The experimental results are presented in Table 1.

6.1 A Nonlinear System of Prey-Predator

Example 14 Consider a nonlinear system of prey-predator, where the population dynamics are described by the following DDE:

$$\begin{aligned} \dot{x}_1(t) &= bx_1(t)b - x_1(t)^2 - 4x_1(t)x_2(t) \\ \dot{x}_2(t) &= 4.8x_1(t - \tau)x_2(t - \tau) - x_2(t - \tau) \end{aligned}$$

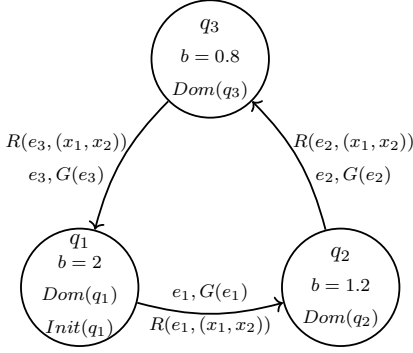
Here, $x_1(t)$ and $x_2(t)$ represent the populations of prey and predator, respectively; b denotes the rate of increase of the prey population; τ accounts for the maturation process of the predator population. We assume $\tau = 0.001$ in this example.

The increase rate b of prey may be influenced by the environment and change between different values. In Fig. 8, a dHA is presented to depict such switch, where each mode corresponds to a specific value of b .

The safe set in all modes is equal to its domain, formally, $S_{q_1} = \text{Dom}(q_1)$, $S_{q_2} = \text{Dom}(q_2)$, $S_{q_3} = \text{Dom}(q_3)$; the target set in q_3 is defined as $T_{q_3} = \{(x_1, x_2) \mid (x_1 - 0.2)^2 + (x_2 - 0.2)^2 \leq 0.01\}$ and the target set in q_1, q_2 is empty.

³ Note in Alg. 4 do not specify which edge to be removed when finding a simple loop, the completeness proof presented here requires enumerating all possibility.

⁴ Some examples are obtained by duplicating their continuous dynamics with different target sets to create the corresponding delay hybrid systems.



$$\begin{aligned}
Dom(q_1) &= \{(x_1, x_2) \mid (x_1 - 0.2)^2 + (x_2 - 0.2)^2 \leq 0.04\}, \\
Init(q_1) &= \{(x_1, x_2) \mid (x_1 - 0.2)^2 + (x_2 - 0.2)^2 \leq 0.04\}, \\
G(e_1) &= \{(x_1, x_2) \mid (x_1 - 0.4)^2 + (x_2 - 0.3)^2 \leq 0.01\}, \\
Dom(q_2) &= \{(x_1, x_2) \mid (x_1 - 0.5)^2 + (x_2 - 0.5)^2 \leq 0.25\}, \\
G(e_2) &= \{(x_1, x_2) \mid (x_1 - 0.1)^2 + (x_2 - 0.5)^2 \leq 0.01\}, \\
Dom(q_3) &= \{(x_1, x_2) \mid (x_1 - 0.3)^2 + (x_2 - 0.3)^2 \geq 0.09\}, \\
G(e_3) &= \{(x_1, x_2) \mid (x_1 - 0.1)^2 + (x_2 - 0.5)^2 \leq 0.01\}
\end{aligned}$$

Fig. 8. The dHA for the prey-predator system

Denote the resulted dHA with Alg. 5 by $\mathcal{H}^r = (Q, X, Dom, F, Init^r, E, G, ST, R^r)$. For simplicity, we use $\mathcal{RA}_{in}(i, j)$ to denote the reach-avoid set approximated by Alg. 1, i.e.,

$$\begin{aligned}
\mathcal{RA}_{in}(1, 1) &:= \text{InRA}(\mathbf{f}_1, Dom(q_1) \cap S_{q_1}, G(e_1) \setminus Dom(q_1)), \\
\mathcal{RA}_{in}(2, 1) &:= \text{InRA}(\mathbf{f}_2, Dom(q_2) \cap S_{q_2}, G(e_2) \setminus Dom(q_2)), \\
\mathcal{RA}_{in}(3, 1) &:= \text{InRA}(\mathbf{f}_3, Dom(q_3) \cap S_{q_3}, G(e_3) \setminus Dom(q_3)), \\
\mathcal{RA}_{in}(3, 0) &:= \text{InRA}(\mathbf{f}_3, Dom(q_3) \cap S_{q_3}, T_{q_3})
\end{aligned}$$

Then, the reset controller we synthesized is given by

$$\begin{aligned}
R^r(e_1, G(e_1)) &= \mathcal{RA}_{in}(2, 1), \\
R^r(e_2, G(e_2)) &= \mathcal{RA}_{in}(3, 0), \\
R^r(e_3, G(e_3)) &= \emptyset, \\
Init^r(q_1) &= Init(q_1) \cap \mathcal{RA}_{in}(1, 1)
\end{aligned}$$

Simulations of the pre-predator system before and after reset controller synthesis is present in Fig. 9 and Fig. 10, respectively. In Fig. 9, it can be observed that the pre-predator system without the synthesized reset controller may infinitely operate within the safe region never entering the target set. In fact, during the progression of the reset controller synthesis, edge e_3 has been disabled from the dHA since all execution paths through q_3 are forced to enter the target set in order to avoid infinitely many iteration among $q_3 \rightarrow q_1 \rightarrow q_2 \rightarrow q_3$. With the synthesized reset map, all continuous evolutions in q_3 will lead to the target set T_{q_3} eventually, meanwhile all execution paths in each mode stay in the safe set. \triangleleft

6.2 More Case Studies

In this subsection, we aim to demonstrate the scalability of our method by applying it to a range of large-scale benchmarks from the literature. The results obtained with our tool on these benchmark examples are presented in Table 1.

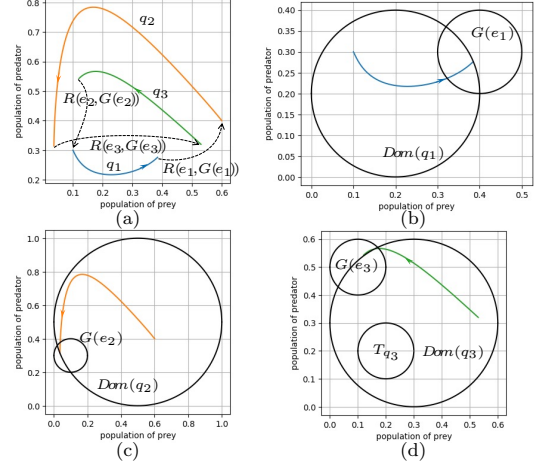


Fig. 9. Simulation of the pre-predator system before reset controller synthesis: Figure (a) shows the simulation of the pre-predator system before reset controller synthesis, where an execution begins from the initial set $Init(q_1)$. The system runs indefinitely within the safe region but does not enter the target set T_{q_3} . The dashed line in Figure (a) represents the reset map used in the simulation. For further clarity, Figures (b), (c), and (d) illustrate the execution in modes q_1 , q_2 , and q_3 , respectively.

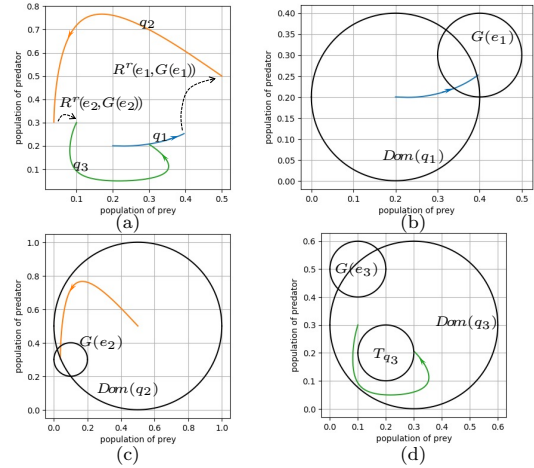


Fig. 10. Simulation of the pre-predator system after reset controller synthesis: Figure (a) presents an execution starting from the initial set $Init^r(q_1)$ and terminating at the target set T_{q_3} . The dashed line in Figure (a) represents the reset map used in the simulation. Figures (b), (c), and (d) provide an illustration of the execution in mode q_1 , q_2 , and q_3 respectively.

Oscillator, is a hybrid damped oscillator similar to the one in Example 2, with more discrete transitions between modes. Low-Pass Filter is taken from [2], which consists of 9 low-pass filters and 14 discrete transitions between different modes. Prey-Predator is a linearized version of the prey-predator system in Example 14 with a larger number of modes and edges. PD Controller is an adaptation of the PD controller presented in [19] and showcases

Table 1
Experimental results for reset controller synthesis

Benchmark	dim	original model		synthesis time		result model	
		modes	edges	time 1	time 2	modes	edges
Oscillator [37]	2	3	4	11.08s	78.64ms	3	3
Low-Pass Filter [2]	2	9	14	44.75s	100.98ms	8	13
Prey-Predator [6]	2	12	28	2m4s	100.14ms	12	27
PD Controller [19]	2	16	31	2m45s	79.88ms	15	20
CWH Equation [21]	4	5	8	23m29s	102.48ms	5	7

dim: the dimension of instant states; modes: the number of modes; edges: the number of discrete transitions; original model: the dHA before synthesizing (i.e., \mathcal{H}); resulted model: the dHA after synthesizing (i.e., \mathcal{H}^r); time 1: the time consumed by mode partition (i.e., Alg. 2); time 2: the time consumed by synthesizing reset controller

a PD controller designed for a self-driving car that can switch between different modes. Lastly, *CWH Equation* is a delay hybrid system utilized to model the relative orbital motion of a chase spacecraft in relation to a reference spacecraft. It can switch between different chase strategies.

The table demonstrates the effectiveness of our method in synthesizing reset controllers for various benchmarks from the literature. The time required for synthesizing is mainly determined by the mode partition step (time 1), which involves in solving a series of SDP problems for each mode with respect to each guard condition. Therefore, more the synthesis time for examples with higher dimension, which also depend on the efficiency of the SDP solver used. The time required to synthesize a reset controller in the first step (time 2) is not sensitive to the size of problems, as the resulted discrete directed diagrams in Table 1 are relatively small in compared with those usually tackled by NetworkX. The advantage of our method for reach-avoid analysis is its ability to handle examples with larger time delay efficiently. Therefore, we do not include the comparison with the method of [37] in the table.

7 Conclusion

In this paper, we provide a constructive method for synthesizing reset controllers for delay hybrid systems, subject to reach-avoid properties. Our approach employs a novel method for inner-approximating reach-avoid sets for polynomial delay differential equations. We then propose a sound and complete method⁵ for synthesizing reset controller. Through experiments on a set of relevant examples from the literature, we demonstrate the effectiveness of our approach.

As future work, we aim to extend our approach to more general delay hybrid systems (HSs) with more complicated vector fields in each mode. Additionally, we plan to investigate the potential of a correct-by-construction framework for HSs by integrating feedback controller

⁵ Under the assumption that RABFals synthesized with SDP-based approaches are correct.

synthesis, switching logic controller synthesis, and reset controller synthesis into a unified approach.

References

- [1] Alessandro Abate, Iury Bessa, Dario Cattaruzza, Lucas Cordeiro, Cristina David, Pascal Kesseli, Daniel Kroening, and Elizabeth Polgreen. Automated formal synthesis of digital controllers for state-space physical plants. In *CAV 2017*, pages 462–482. Springer, 2017.
- [2] Matthias Althoff and Dmitry Grebenyuk. Implementation of interval arithmetic in {CORA} 2016. In *Proc. of the 3rd International Workshop on Applied Verification for Continuous and Hybrid Systems*, pages 91–105, 2016.
- [3] Aaron D Ames, Xiangru Xu, Jessy W Grizzle, and Paulo Tabuada. Control barrier function based quadratic programs for safety critical systems. *IEEE Transactions on Automatic Control*, 62(8):3861–3876, 2016.
- [4] Erling D Andersen, Cornelis Roos, and Tamas Terlaky. On implementing a primal-dual interior-point method for conic quadratic optimization. *Mathematical Programming*, 95:249–277, 2003.
- [5] Eugene Asarin, Olivier Bournez, Thao Dang, Oded Maler, and Amir Pnueli. Effective synthesis of switching controllers for linear systems. *Proceedings of the IEEE*, 88(7):1011–1025, 2000.
- [6] Yunjun Bai, Ting Gan, Li Jiao, Bican Xia, Bai Xue, and Naijun Zhan. Switching controller synthesis for delay hybrid systems under perturbations. In *HSCC 2021*, pages 1–11, 2021.
- [7] O Beker, CV Hollot, Q Chen, and Y Chait. Stability of a reset control system under constant inputs. In *ACC 1999*, volume 5, pages 3044–3045. IEEE, 1999.
- [8] Calin Belta, Boyan Jordanov, and Ebru Aydin Gol. *Formal methods for discrete-time dynamical systems*, volume 15. Springer, 2017.
- [9] Michael S Branicky. Stability of switched and hybrid systems. In *CDC 1994*, volume 4, pages 3498–3503. IEEE, 1994.
- [10] Anupam Chattopadhyay and Kwok-Yan Lam. Security of autonomous vehicle as a cyber-physical system. In *2017 7th International Symposium on Embedded Computing and System Design (ISED)*, pages 1–6. IEEE, 2017.
- [11] John C Clegg. A nonlinear integrator for servomechanisms. *Transactions of the American Institute of Electrical Engineers, Part II: Applications and Industry*, 77(1):41–42, 1958.

- [12] Nilanjan Dey, Amira S Ashour, Fuqian Shi, Simon James Fong, and João Manuel RS Tavares. Medical cyber-physical systems: A survey. *Journal of medical systems*, 42:1–13, 2018.
- [13] Olaf Diegel, Aparna Badve, Glen Bright, Johan Potgieter, and Sylvester Tlale. Improved mecanum wheel design for omni-directional robots. In *Proc. 2002 Australasian conference on robotics and automation, Auckland*, pages 117–121, 2002.
- [14] Shenghua Feng, Mingshuai Chen, Bai Xue, Sriram Sankaranarayanan, and Naijun Zhan. Unbounded-time safety verification of stochastic differential dynamics. In *CAV 2020*, volume 12225 of *Lecture Notes in Computer Science*, pages 327–348. Springer, 2020.
- [15] Martin Fränzle, Mingshuai Chen, and Paul Kröger. In memory of oded maler: automatic reachability analysis of hybrid-state automata. *ACM SIGLOG News*, 6(1):19–39, 2019.
- [16] Emilia Fridman. *Introduction to time-delay systems: Analysis and control*. Springer, 2014.
- [17] Emilia Fridman, Michel Dambrine, and Nima Yeganefer. On input-to-state stability of systems with time-delay: A matrix inequalities approach. *Automatica*, 44(9):2364–2369, 2008.
- [18] Antoine Girard. Controller synthesis for safety and reachability via approximate bisimulation. *Automatica*, 48(5):947–953, 2012.
- [19] Eric Goubault, Sylvie Putot, and Lorenz Sahlmann. Inner and outer approximating flowpipes for delay differential equations. In *CAV 2018*, pages 523–541. Springer, 2018.
- [20] Yuqian Guo, Youyi Wang, Lihua Xie, and Jinchuan Zheng. Stability analysis and design of reset systems: Theory and an application. *Automatica*, 45(2):492–497, 2009.
- [21] Baisravan HomChaudhuri, Meeko Oishi, Matt Shubert, Morgan Baldwin, and R Scott Erwin. Computing reach-avoid sets for space vehicle docking under continuous thrust. In *CDC 2016*, pages 3312–3318. IEEE, 2016.
- [22] Kyle Hsu, Rupak Majumdar, Kaushik Mallik, and Anne-Kathrin Schmuck. Multi-layered abstraction-based controller synthesis for continuous-time systems. In *HSCC 2018*, pages 120–129, 2018.
- [23] Zhenqi Huang, Chuchu Fan, and Sayan Mitra. Bounded invariant verification for time-delayed nonlinear networked dynamical systems. *Nonlinear Analysis: Hybrid Systems*, 23:211–229, 2017.
- [24] Adam K Kiss, Tamas G Molnar, Aaron D Ames, and Gábor Orosz. Control barrier functionals: Safety-critical control for time delay systems. *arXiv preprint arXiv:2206.08409*, 2022.
- [25] J Lfberg. A toolbox for modeling and optimization in matlab. In *Proceedings of the Conference on Computer-Aided Control System Design (CACSD) p*, volume 284289, 2004.
- [26] Petter Nilsson, Necmiye Ozay, and Jun Liu. Augmented finite transition systems as abstractions for control synthesis. *Discrete Event Dynamic Systems*, 27:301–340, 2017.
- [27] Stephen Prajna and Ali Jadbabaie. Methods for safety verification of time-delay systems. In *CDC 2005*, pages 4348–4353. IEEE, 2005.
- [28] Stephen Prajna, Antonis Papachristodoulou, Peter Seiler, and Pablo A Parrilo. Sostools and its control applications. *Positive polynomials in control*, pages 273–292, 2005.
- [29] Christophe Prieur, Isabelle Queinnec, Sophie Tarbouriech, Luca Zaccarian, et al. Analysis and synthesis of reset control systems. *Foundations and Trends® in Systems and Control*, 6(2-3):117–338, 2018.
- [30] Ragunathan Rajkumar, Insup Lee, Lui Sha, and John Stankovic. Cyber-physical systems: the next computing revolution. In *DAC 2010*, pages 731–736, 2010.
- [31] Gunther Reissig, Alexander Weber, and Matthias Rungger. Feedback refinement relations for the synthesis of symbolic controllers. *IEEE Transactions on Automatic Control*, 62(4):1781–1796, 2016.
- [32] Ricardo G Sanfelice. *Hybrid feedback control*. Princeton University Press, 2021.
- [33] Paulo Tabuada. *Verification and control of hybrid systems: a symbolic approach*. Springer Science & Business Media, 2009.
- [34] Ankur Taly, Sumit Gulwani, and Ashish Tiwari. Synthesizing switching logic using constraint solving. *International journal on software tools for technology transfer*, 13(6):519–535, 2011.
- [35] Claire J Tomlin, John Lygeros, and S Shankar Sastry. A game theoretic approach to controller design for hybrid systems. *Proceedings of the IEEE*, 88(7):949–970, 2000.
- [36] Henry Wolkowicz, Romesh Saigal, and Lieven Vandenbergh. *Handbook of semidefinite programming: theory, algorithms, and applications*, volume 27. Springer Science & Business Media, 2012.
- [37] Bai Xue, Yunjun Bai, Naijun Zhan, Wenyu Liu, and Li Jiao. Reach-avoid analysis for delay differential equations. In *CDC 2021*, pages 1301–1307. IEEE, 2021.
- [38] Bai Xue, Peter Nazier Mosaad, Martin Fränzle, Mingshuai Chen, Yangjia Li, and Naijun Zhan. Safe over-and under-approximation of reachable sets for delay differential equations. In *FORMATS 2017*, pages 281–299. Springer, 2017.
- [39] Hengjun Zhao, Naijun Zhan, and Deepak Kapur. Synthesizing switching controllers for hybrid systems by generating invariants. *Theories of Programming and Formal Methods: Essays Dedicated to Jifeng He on the Occasion of His 70th Birthday*, pages 354–373, 2013.
- [40] Hengjun Zhao, Naijun Zhan, Deepak Kapur, and Kim G Larsen. A” hybrid” approach for synthesizing optimal controllers of hybrid systems: A case study of the oil pump industrial example. *FM*, 12:471–485, 2012.
- [41] Pengcheng Zhao, Shankar Mohan, and Ram Vasudevan. Optimal control of polynomial hybrid systems via convex relaxations. *IEEE Transactions on Automatic Control*, 65(5):2062–2077, 2019.
- [42] Liang Zou, Martin Fränzle, Naijun Zhan, and Peter Nazier Mosaad. Automatic verification of stability and safety for delay differential equations. In *CAV*, volume 9207 of *Lecture Notes in Computer Science*, pages 338–355. Springer, 2015.